NASA Technical Memorandum 105804

Controller Partitioning for Integrated Flight/ Propulsion Control Implementation

Sanjay Garg
Lewis Research Center
Cleveland, Ohio

Prepared for the
1992 American Control Conference
sponsored by the American Automatic Control Council
Chicago, Illinois, June 24–26, 1992

NASA

CONTROLLER PARTITIONING FOR INTEGRATED FLIGHT/PROPULSION CONTROL IMPLEMENTATION

Sanjay Garg
NASA Lewis Research Center
Advanced Control Technology Branch
Cleveland, OH 44135

Abstract

The notion of partitioning a centralized controller into a decentralized, hierarchical structure suitable for integrated flight/propulsion control (IFPC) implementation is discussed. A systematic procedure is developed for determining partitioned airframe and engine subsystem controllers (subcontrollers), with the desired interconnection structure, that approximate the closed-loop performance and robustness characteristics of a given centralized controller. The procedure is demonstrated by application to IFPC design for a Short Take-Off and Vertical Landing (STOVL) aircraft in the landing approach to hover transition flight phase.

Introduction

Large interconnected systems often exhibit a significant amount of coupling between the various subsystems thus requiring an integrated approach to controller design. Short Take-Off and Vertical Landing (STOVL) aircraft are examples of such systems. In conventional aircraft, the propulsion system mainly provides control of the longitudinal axis through generation of axial thrust. However, in STOVL aircraft the forces and moments generated by the propulsion system provide the control and maneuvering capabilities for all axes of the aircraft at low speeds thus creating the need for Integrated Flight/Propulsion Control (IFPC) system design.

One approach to integrated control design for large interconnected systems is to "partition" the overall system into loosely coupled subsystems and then do a decentralized control design considering one subsystem at a time. A survey of decentralized control design techniques can be found in Ref. [1] and an example application of decentralized control design techniques to IFPC design is available in Ref. [2]. Although the decentralized approach to integrated control design is intuitively appealing in that it results in low-order, independently implementable subsystem controllers (referred to as "subcontrollers"), it has the disadvantage that it does not easily account for all the interactions between the various subsystems. The strengths and weaknesses of a decentralized, hierarchical approach to IFPC design are further discussed in Ref. [3].

Another approach to integrated control design is to design a centralized controller considering the integrated plant with all its interconnections. An IFPC design based on a centralized approach is discussed in Ref. [4]. Although such an approach yields an "optimal" design since it accounts for all the subsystem interactions, it results in a high-order controller which is difficult to implement and validate. Often the design, manufacture and testing of different subsystems are performed by different companies which are accountable for individual subsystem performance. For instance, in an aircraft design it is the responsibility of the engine manufacturer to ensure that the propulsion system will provide the desired performance when installed in the airframe. The subsystem validation is accomplished through extensive testing with an independent subcontroller. The testing of and accountability for performance of each subsystem can be a formidable task with a centralized controller since closed-loop performance evaluation would require all the subsystems to be assembled without prior independent testing. The strengths and weaknesses of a centralized approach to IFPC design are further discussed in Ref. [5].

An approach to integrated control design which combines the "best" aspects of the centralized and decentralized approaches has been developed in Ref. [6]. This approach consists of first designing a centralized controller considering the airframe and propulsion systems as one integrated system, and then partitioning the centralized controller into decentralized subcontrollers with a specified interconnection structure. By partitioning here is meant approximating the high-order centralized controller with two or more lower order subcontrollers with a specified coupling structure, such that the closed-loop performance and robustness characteristics of the centralized controller are matched by the partitioned subcontrollers. The centralized control design accounts for all the subsystem interactions at the initial design stage and provides a baseline for the "best" achievable performance with a fully integrated system. The partitioning results in easy to implement subcontrollers that allow for independent subsystem validation and also allow for the system nonlinearities to be considered in detail at the subsystem level. A meaningful trade-off between subcontroller complexity and achievable performance for the integrated system can be performed by evaluating various controller partitionings of different levels of complexity against the performance baseline established with the centralized controller.

The objectives of this paper are to describe a systematic stepwise procedure for

determining partitioned subcontrollers that closely match the performance achieved with the centralized controller and to demonstrate the procedure by application to a STOVL aircraft IFPC design problem. In the following, the specific partitioning structure to be considered is first described. The controller partitioning procedure is then presented followed by a discussion of the STOVL aircraft IFPC design example.

Controller Partitioning Problem Description

The desired structure of the controller partitioning will depend on the coupling between the various subsystems and on practical considerations related to integration of the independently controlled subsystems. As pointed out in Ref. [2], the most suitable control structure for the IFPC problem is hierarchical with the airframe (flight) controller generating commands for the aerodynamic control surfaces as well as for the propulsion subsystem. This decentralized, hierarchical control structure is shown in Fig. 1 where the subscripts and superscripts "a" and "e" refer to airframe and propulsion system (engine) quantities, respectively, subscript "c" refers to commands, and the variables $\bar{z}$ are the controlled outputs of interest with $\bar{e}$ being the corresponding errors. The intermediate variables $\bar{z}_{ea}$ represent propulsion system quantities that affect the airframe, for example propulsion system generated forces and moments.

The controller partitioning problem of Fig. 1 can be stated as follows:

Given: A centralized controller K(s) s.t.

$$\bar{u}(s) = K(s)\begin{bmatrix}\bar{e}(s)\\ \bar{y}(s)\end{bmatrix}, \text{ where } \bar{u} = \begin{bmatrix}\bar{u}_a\\ \bar{u}_e\end{bmatrix}, \bar{e} = \begin{bmatrix}\bar{e}_a\\ \bar{e}_e\end{bmatrix}, \text{ and } \bar{y} = \begin{bmatrix}\bar{y}_a\\ \bar{y}_e\end{bmatrix}, \tag{1}$$

and a particular set of the interface variables $\bar{z}_{ea}$,

Find: Decentralized airframe and engine subcontrollers, $K^a(s)$ and $K^e(s)$, respectively, with

$$\begin{bmatrix}\bar{u}_a(s)\\ \bar{z}_{ea_c}(s)\end{bmatrix} = K^a(s)\begin{bmatrix}\bar{e}_a(s)\\ \bar{y}_a(s)\end{bmatrix}, \text{ and } \bar{u}_e(s) = K^e(s)\begin{bmatrix}\bar{e}_{ea}(s)\\ \bar{e}_e(s)\\ \bar{y}_e(s)\end{bmatrix} \tag{2}$$

So that: The closed-loop performance and robustness with the subcontrollers $K^a(s)$ and $K^e(s)$ match those with the centralized controller K(s) to a desired accuracy. Furthermore, the engine subcontroller $K^e(s)$ should have the structure of a command tracking controller for the interface variables $\bar{z}_{ea}$ to allow for independent check-out of the propulsion system.

In the above problem statement, the elements of $\bar{z}_a$ and $\bar{z}_e$ are mutually exclusive and correspond to the traditional definition of airframe and engine variables. For example, $\bar{z}_a$ would consist of aircraft velocity, pitch and roll attitudes and rates etc. while $\bar{z}_e$ would consist of engine rotor speeds, pressure ratios etc. The elements of $\bar{u}_a$ and $\bar{u}_e$ are also mutually exclusive to allow for independent control implementation and subsystem validation, i.e. the subcontrollers cannot both have authority over the same control actuator. The partitioning of $\bar{u}$ into $\bar{u}_a$ and $\bar{u}_e$ is based on control effectiveness evaluation in terms of capability to "directly" control $\bar{z}_a$ or $\bar{z}_e$ and not necessarily on physical control actuator location. For example, for aircraft equipped with thrust vectoring nozzles, the thrust vectoring control will be part of $\bar{u}_a$ because thrust vectoring "directly" affects aircraft velocity and angular position and rates. Although some engine controls affect airframe outputs $\bar{z}_a$ upon integrating the subsystems, this effect is mainly through the interface variables $\bar{z}_{ea}$. For example, an increase in fuel flow results in an increase in the thrust generated by the engine which in turn results in an increase in the aircraft velocity. Therefore such engine controls will be more appropriately included in $\bar{u}_e$. The elements of feedback variables $\bar{y}_a$ and $\bar{y}_e$ need not be mutually exclusive or correspond to the traditional definition of airframe and engine outputs. For instance, sideslip and sideslip rate feedback could be used not only in the airframe subcontroller for augmentation of the aircraft lateral/directional dynamics, but also in the engine subcontroller to estimate inlet distortion due to large maneuvers and provide active control of engine fan/compressor surge margin. It is worth noting, however, that including an output in both $\bar{y}_a$ and $\bar{y}_e$ might impose additional requirements on subsystem control implementation and validation.

Procedure for Controller Partitioning

Let the controlled plant $\hat{G}(s)$ be of the form

$$\hat{G}(s) = \begin{bmatrix} G(s) \\ \hat{G}_{ea}(s) \end{bmatrix} \tag{3}$$

with

$$\begin{bmatrix} \begin{Bmatrix} \bar{z}_a \\ \bar{y}_a \end{Bmatrix} \\ \begin{Bmatrix} \bar{z}_e \\ \bar{y}_e \end{Bmatrix} \end{bmatrix} = G(s)\bar{u} \; ; \; G(s) = \begin{bmatrix} G_{aa}(s) & G_{ae}(s) \\ G_{ea}(s) & G_{ee}(s) \end{bmatrix}$$

and

$$\bar{z}_{ea} = \hat{G}_{ea}(s)\,\bar{u}(s) \; ; \; \hat{G}_{ea}(s) = [G^a_{ea}(s) \; G^e_{ea}(s)],$$

and the centralized controller K(s) be of the form

$$\begin{bmatrix} \bar{u}_a \\ \bar{u}_e \end{bmatrix} = K(s) \begin{bmatrix} \begin{Bmatrix} \bar{e}_a \\ \bar{y}_a \end{Bmatrix} \\ \begin{Bmatrix} \bar{e}_e \\ \bar{y}_e \end{Bmatrix} \end{bmatrix} ; \; K(s) = \begin{bmatrix} K_{aa}(s) & K_{ae}(s) \\ K_{ea}(s) & K_{ee}(s) \end{bmatrix} \tag{4}$$

where the partitioning of $\bar{u}$ is as in (1) and the columns of K(s) have been rearranged to reflect grouping of the airframe and engine controller inputs. The subcontrollers $K^a(s)$ and $K^e(s)$ obtained by application of the partitioning procedure to be presented in this paper are of the form

$$K^a(s) = [I \;\; K^{lead}(s)]\,\bar{K}^a(s) \; ; \; K^e(s) = [K^e_{ea}(s) \;\; K^e_e(s)]$$

where I is an appropriately dimensioned identity matrix. The structure of the subcontrollers is shown in Fig. 2. The steps in determining the four blocks, $\tilde{K}^a(s)$, $K^{lead}(s)$, $K^c_{ea}(s)$ and $K^c_e(s)$ are discussed next.

Step 1; $K^c_e(s)$: Obtain a state-space representation of the $K^c_e(s)$ block of the engine subcontroller as a reduced order approximation of the $K_{ee}(s)$ block of the centralized controller. Any suitable model/controller order reduction technique, such as the internally balanced realization approach [7], can be used for this step. In order to reduce subcontroller complexity, it is important to keep the order of $K^c_e(s)$ as low as possible while obtaining a good match with the input/output characteristics of the corresponding centralized controller block $K_{ee}(s)$.

Step 2; Design Specifications for $K^c_{ea}(s)$: Analyze the response of the interface variables $\bar{z}_{ea}$ to airframe controlled variable commands $\bar{z}_{a_c}$ with the centralized controller to determine the bandwidth requirements on the engine subsystem for tracking the interface variable commands $\bar{z}_{ea_c}$ generated by the partitioned airframe subcontroller. Here, bandwidth ω_{ea_i} is defined as the frequency at which the magnitude of the closed-loop frequency response from a commanded variable to the corresponding response, $\left|\frac{z^i_{ea}}{z^i_{ea_c}}(j\omega)\right|$ for example, is -3 dB. One way to determine these requirements is to study the closed-loop frequency response $T^{ea_i}_{a_c}(j\omega)$ from all the airframe commands to each individual element z^i_{ea} of the interface variables with the centralized controller. A suitable minimum requirement on the tracking bandwidth ω_{ea_i} for the engine subsystem, in order to match the performance with the centralized controller, is that ω_{ea_i} be such that $\sigma[T^{ea_i}_{a_c}(j\omega)] \ll 1$ for $\omega > \omega_{ea_i}$. Heuristically, this argument implies that the demand for response in interface variable z^i_{ea} required to track the airframe commands $\bar{z}_{a_c}$ will "roll-off" prior to loss

in the capability of the engine subcontroller to track the corresponding command $z^i_{ea_c}$.

Note that in general there will be other limits on the minimum required tracking bandwidth for the interface variables imposed by subsystem specific performance requirements such as disturbance rejection, performance robustness to low frequency model variations etc. Furthermore, control actuation limits and requirement of robustness to high frequency modelling errors will impose limits on the maximum achievable tracking bandwidth for the engine subsystem. It is important to consider all these requirements in generating the design specifications for $K^e_{ea}(s)$.

As an aside, it is worthwhile here to note the difference between the above procedure for generating design specifications for the engine subcontroller and the "subsystem specification" generation procedure of the decentralized approach to IFPC design as discussed in Ref. [2]. The above procedure generates specifications on the *nominal* command tracking response that should be achieved by the engine subsystem for the integrated system closed-loop *performance* with the decentralized controllers to be comparable to that with the centralized controller. The procedure of Ref. [2] *assumes* some nominal achievable tracking response capability with the engine subsystem and uses the "mission level" control design to generate bounds around the *assumed nominal* such that the integrated system closed-loop *stability* is guaranteed.

Step 3; Design of $K^e_{ea}(s)$: Design $K^e_{ea}(s)$ to meet the $\bar{z}_{ea_c}$ tracking specifications, derived in Step 2. Another requirement that might be placed on the engine subcontroller $K^e(s)$ is to provide decoupling between $\bar{z}_e$ and $\bar{z}_{ea}$ responses. Since the centralized control design objective is to provide decoupled command tracking of $\bar{z}_a$ and $\bar{z}_{e_c}$, and since the interface variables affect the airframe controlled outputs, $\bar{z}_a$, the $K_{ee}(s)$ block of a properly designed centralized controller, hence $K^e_e(s)$ block of $K^e(s)$, will be such that the engine subsystem closed-loop $\bar{z}_{ea}$ response to $\bar{z}_{e_c}$ is "small". Designing $K^e_{ea}(s)$ to provide decoupled command tracking of $\bar{z}_{ea}$ without "excessive" disturbance in $\bar{z}_e$ will then result in an overall $K^e(s)$ which provides decoupled command tracking

of $\bar{z}_{ea}$ and $\bar{z}_{e}$. Any control synthesis technique that allows for formulating a mixed command tracking and regulation control problem can be used for the design of $K^{c}_{ea}(s)$.

Step 4; $\hat{K}^{a}(s)$: With the engine subsystem loop closed using the centralized controller, as shown in Fig. 3, obtain a state-space representation for $\hat{K}^{a}(s)$ as a reduced-order approximation of the $\begin{bmatrix} \bar{e}_a \\ \bar{y}_a \end{bmatrix} \rightarrow \begin{bmatrix} \bar{u}_a \\ \bar{z}_{ea} \end{bmatrix}$ response with the centralized controller. An expression for this response can be obtained using algebraic manipulation of the various sub-blocks of the centralized controller and the engine subsystem given in equations (4) and (3) respectively. Also, with modern control design software tools which allow graphical block diagram manipulation, for example see Ref. [8], a state-space representation of the $\begin{bmatrix} \bar{e}_a \\ \bar{y}_a \end{bmatrix} \rightarrow \begin{bmatrix} \bar{u}_a \\ \bar{z}_{ea} \end{bmatrix}$ response can be obtained directly from a block diagram of the type shown in Fig. 3.

Step 5; $K^{lead}(s)$: Design $K^{lead}(s)$ to be a lead filter to compensate for the limited $\bar{z}_{ea_c}$ tracking bandwidth of the engine subsystem. Note that $\hat{K}^{a}(s)$, as obtained in Step 4, generates $\bar{z}_{ea_{des}}$, the desired response in the interface variables to airframe controlled variable commands such that the integrated system achieves the specified tracking and decoupling response. If $\bar{z}_{ea_{des}}$ were used directly as commands for the interface variables, $\bar{z}_{ea_c}$, then the actual $\bar{z}_{ea}$ response with the partitioned subcontrollers would lag the desired response $\bar{z}_{ea_{des}}$ due to the limited tracking bandwidth of the engine subsystem thus resulting in deterioration in integrated system performance. In general, there will be a design trade-off based on practical considerations between the amount of lead compensation in $K^{lead}(s)$ and the $\bar{z}_{ea_c}$ tracking bandwidth of the engine subsystem. High lead compensation is undesirable as it can result in saturation of the engine actuators due to command magnification, whereas low lead compensation will require large $\bar{z}_{ea_c}$

tracking bandwidth. Since the $K^{c}_{ea}(s)$ portion of the engine controller provides decoupled tracking of $\bar{z}_{ea_c}$, $K^{lead}(s)$ can be simply be of the form

$$K^{lead}(s) = \text{diag}\left[\frac{s+a_i}{a_i}\,\frac{b_i}{s+b_i}\right], \quad a_i<b_i \tag{5}$$

with a_i and b_i chosen based on the amount of lead desired in z^{i}_{ea}.

Using plant information, the decentralized subcontrollers as obtained above can be "assembled" into an *equivalent* centralized controller $\tilde{K}(s)$ having the same input/output form as the centralized controller K(s) of equation (4), with

$$\tilde{K}(s) = \begin{bmatrix} \tilde{K}_{aa}(s) & 0 \\ \tilde{K}_{ea}(s) & \tilde{K}_{ee}(s) \end{bmatrix} \tag{6}$$

The $\begin{bmatrix} \tilde{K}_{aa}(s) \\ \tilde{K}_{ea}(s) \end{bmatrix}$ portion of $\tilde{K}(s)$ approximates the $\begin{bmatrix} K_{aa}(s) \\ K_{ea}(s) \end{bmatrix}$ portion of K(s) via the combined effect of $\tilde{K}^{a}(s)$, $K^{lead}(s)$ and $K^{c}_{ea}(s)$, and $\tilde{K}_{ee}(s)$ ($=K^{c}_{e}(s)$ of Step 1) approximates $K_{ee}(s)$. For most aircraft, even STOVL configurations, the coupling from airframe control inputs to engine outputs, i.e. $G_{ea}(s)$ and $G^{a}_{ea}(s)$ in (3), is "small". Furthermore, the coupling in this direction is generally an undesirable disturbance on the engine dynamics rather than an effective input for control of engine outputs. For such systems, a properly designed centralized controller will be such that the $K_{ae}(s)$ block is "small". So, although the partitioning structure of Fig. 1 does not include an equivalent $\tilde{K}_{ae}(s)$ block, the centralized controller closed-loop performance can still be matched with the partitioned subcontrollers. However, controller partitioning for systems which have strong coupling from airframe control inputs to engine outputs will necessitate considering appropriate modifications to the partitioned control structure.

Controller Partitioning Example

The controller partitioning procedure discussed above was applied to the centralized IFPC design for a STOVL aircraft in the decelerating transition during approach to hover landing flight phase. A schematic diagram of the aircraft is shown in Fig. 4. The aircraft is powered by a two-spool turbofan engine and is equipped with the following control effectors: left and right elevons used collectively as elevator and differentially as ailerons; rudder; ejectors to provide propulsive lift at low speeds and hover; a 2D-CD (two dimensional convergent-divergent) vectoring aft nozzle; a vectoring ventral nozzle for pitch control and lift augmentation during transition; and jet reaction control systems (RCS) for pitch, roll and yaw control during transition and hover. Engine compressor bleed flow (WB3) is used for the RCS thrusters and the mixed engine flow is used as the primary ejector flow. The aircraft and engine model and the design of the centralized controller for a linear integrated design model are discussed in detail in Refs. [8, 9]. The centralized controller was partitioned into decoupled lateral and longitudinal-plus-engine subcontrollers as discussed in Ref. [9]. In the following, the vehicle model is first summarized, and the partitioning of the longitudinal-plus-engine controller into separate longitudinal and engine subcontrollers with the decentralized, hierarchical control structure is then discussed in detail.

The linear integrated aircraft longitudinal dynamics and engine dynamics small perturbation model is of the form

$$\dot{\bar{x}} = A\bar{x} + B\bar{u} \tag{7}$$

where the state vector is

$$\bar{x} = [N2,N25,Tmhpc,Tmpc,Tmhpt,Tmlpt,u,w,q,\theta,h]^T$$

with

- N2 = Engine Fan Speed, rpm
- N25 = High Pressure Compressor Speed, rpm
- Tmhpc = High Press. Compressor Metal Temp., °R
- Tmpc = Burner Metal Temp., °R
- Tmhpt = High Pressure Turbine Metal Temp., °R
- Tmlpt = Low Pressure Turbine Metal Temp., °R.
- u = Axial Velocity, ft/s
- w = Vertical Velocity, ft/s
- q = Pitch Rate, rad/s
- θ = Pitch Attitude, rad
- h = Altitude, ft

The control inputs partitioned into airframe and engine control inputs are

$$\bar{u}_a = [\delta e, AQR, ANG79, ANG8]^T$$
$$\bar{u}_e = [WF, A8, ETA, A78]^T$$

with

- δe = Elevator Deflection, deg
- AQR = Pitch RCS Area, in^2
- ANG79 = Ventral Nozzle Vectoring Angle, deg
- ANG8 = Aft Nozzle Vectoring Angle, deg
- WF = Fuel Flow Rate, lbm/hr
- A8 = Aft Nozzle Area, in^2
- ETA = Ejector Butterfly Angle, deg
- A78 = Ventral Nozzle Area, in^2

The controlled outputs for the airframe and engine systems are

$$\bar{z}_a = [Vv, Qv, \gamma]^T \quad ; \quad \bar{z}_e = N2$$

where $Vv = \dot{V} + 0.1V$, $Qv = q + 0.3\theta$ with

- V = True Airspeed, ft/s
- $\dot{V}$ = Acceleration Along Flight Path, ft/s^2
- γ = Flight Path Angle, deg

and the other outputs as discussed under state description with units of q and θ in degrees. As discussed in Ref. [8], the above choice of $\bar{z}_a$ corresponds to providing the pilot with an acceleration command velocity hold system in the forward axis, pitch rate command attitude hold system in the pitch axis and direct command of the flight path angle for vertical axis control. The choice of $\bar{z}_e$ allows for setting the engine operating point independent of the aircraft maneuver.

The inputs to the airframe and the engine controllers are the tracking errors $\bar{e}_a$ and $\bar{e}_e$ corresponding to $\bar{z}_a$ and $\bar{z}_e$ respectively, and the measurement feedbacks

$$\bar{y}_a = [V, \dot{V}, \theta, q]^T \quad ; \quad \bar{y}_e = [N2, WB3]^T$$

where WB3 is the compressor bleed flow demanded by the RCS control. Since the compressor bleed flow is always positive, it is given by $WB3 = K_Q|AQR|$.

The interface from the propulsion system model to the airframe model is defined by the gross thrust from the three engine nozzle systems, i.e.

$$\bar{z}_{ea} = [FG9, FGE, FGV]^T$$

where

FG9 = Aft Nozzle Gross Thrust, lbf
FGE = Ejector Gross Thrust, lbf
FGV = Ventral Nozzle Gross Thrust, lbf.

Extensive evaluation of the 10th order longitudinal-plus-engine centralized controller [9] indicated that the controller provides decoupled command tracking of the airframe and engine controlled outputs up to the desired bandwidths within actuator constraints, and also meets stability robustness requirements. The plant system matrix is listed in the Appendix. Prior to applying the partitioning procedure, the interface variables and the inputs and outputs of the longitudinal-plus-engine controller were normalized by appropriate scaling factors which are also listed in the Appendix. All of the discussion in the following steps is with reference to the normalized systems.

Step 1; $K_e^c(s)$: Using internally balanced realization model reduction techniques, $K_e^c(s)$ was obtained as a 4th order approximation of the corresponding $K_{ec}(s)$ portion of the longitudinal-plus-engine subcontroller. The maximum and minimum singular values of $K_{ec}(s)$ and $K_e^c(s)$ are compared in Fig. 5 and indicate a good match between the two controller transfer matrices.

Step 2; Design Specifications for $K_{ea}^c(s)$: The singular values of the frequency responses from all the airframe commands to each of the gross thrusts, FG9, FGE and FGV, for the longitudinal-plus-engine controller are shown in Fig. 6. Note that the demand in ejector thrust is more severe than the demand in aft and ventral nozzle thrusts for tracking the airframe commands because of the need for propulsive lift. The demand for all the thrusts rolls off near 1 rad/s and is sufficiently small (< 0.4) for frequencies above 4.5 rad/s. Thus, for the design of K_{ea}^c, a tracking bandwidth specification of 4.5 rad/s for each of the three gross thrusts would be adequate to avoid any significant deterioration in the tracking of the airframe commands with the partitioned subcontrollers. This tracking bandwidth specification is also adequate for rejection of the disturbance due to RCS bleed flow demand and provides robustness to variations in engine dynamics over the transition flight envelope as well as to high frequency modelling uncertainties.

Step 3; Design of $K_{ea}^{e}(s)$: Using a mixed sensitivity H_∞ control synthesis formulation [10] with the 6th order engine subsystem as the design plant, a controller was designed for decoupled tracking of the three thrust commands and fan speed regulation. The sensitivity weights and the complementary sensitivity weights for each of the three thrusts were chosen to reflect the tracking bandwidth requirement of 4.5 rad/s and incorporate robustness to high-frequency unmodelled dynamics. These weights were all chosen to be first order to simplify the control synthesis. The fan speed regulation criterion was reflected in the control synthesis by penalizing the N2 response to thrust commands with a constant weighting. First-order approximations for the 4 engine actuators were also included in the H_∞ control design plant to reflect control actuation limits in the control design by weighting control and control rates. The resulting 16th order controller with the three thrust tracking errors as inputs was reduced to 3rd order using internally balanced realization. This 3rd order $K_{ea}^{e}(s)$ basically consists of three integrators indicating that a proportional plus integral (PI) controller could be designed to adequately meet the design requirements for $K_{ea}^{e}(s)$.

The partitioned engine controller obtained by combining $K_{e}^{e}(s)$ and $K_{ea}^{e}(s)$ provides decoupled tracking of the FG9, FGE, FGV and N2 commands for the engine subsystem. An example closed-loop response of the engine subsystem to a step command of 1000 lbf in FGE is shown in Fig. 7. The nominal (trim) value for the three thrusts and the fan speed are 2400 lbf, 4300 lbf, 6500 lbf, and 7700 rpm, respectively. The plots shown in Fig. 7 indicate steady-state tracking of FGE_c with fast time response and very small disturbances from the nominal values in the FG9, FGV and N2 responses.

Step 4; $\tilde{K}^{a}(s)$: Using internally balanced realization based model reduction, $\tilde{K}^{a}(s)$ was obtained as a 9th order approximation of the 16th order response of the longitudinal-plus-engine controller with the engine subsystem loop closed, as shown in Fig. 3. The maximum and minimum singular values for the 16th order and 9th order frequency responses are shown in Fig. 8.

Step 5; $K^{lead}(s)$: The lead compensation for each of the gross thrust commands was chosen to be

$$K_i^{lead}(s) = \frac{s+4.5}{4.5}\,\frac{12}{s+12}$$

resulting in an effective bandwidth of 12 rad/s for each of the $z^i_{ca_{des}} \rightarrow z^i_{ca}$ responses.

The system matrices for the partitioned subcontroller components $K_c^c(s)$, $K_{ca}^a(s)$, and $\tilde{K}^a(s)$ are listed in the Appendix. Comparisons were performed between the closed-loop responses with the centralized (longitudinal-plus-engine) and the partitioned subcontrollers. An example comparison for step flight path command (γ_c) is shown in Fig. 9. The trim values for V, θ, γ, and N2 are 135 ft/s, 7 deg, -3 deg and 7700 rpm, respectively. So the plots in Fig. 9(a) indicate that the partitioned controllers maintain the flight path tracking and decoupling of velocity, pitch attitude and fan speed achieved by the centralized controller. Although there is increased coupling in the pitch response with the partitioned controllers, the pitch disturbance from the nominal is still quite small considering the "large" flight path command. The thrust responses shown in Fig. 9(b) indicate the similarity in the thrust requirements for tracking the flight path angle command with the centralized and partitioned controllers, and also demonstrate the effect of lead compensation ($\tilde{K}^{lead}(s)$) in the airframe controller. The control ($\bar{u}$) requirements with the partitioned controllers were also quite similar to those with the centralized controller for step commands in all the controlled variables.

The results presented so far have focused on comparing the performance achieved with the optimized subcontrollers with that achieved with the centralized controller. Robustness issues are also of importance in practical control design. Robustness analysis was performed using structured singular values for gain and phase variations occurring at the controlled outputs and the results are shown in Fig. 10 for the centralized and partitioned controller closed-loop systems. The procedure for creating the interconnection matrix to perform gain and phase margin robustness analysis using structured singular values is documented in Ref. [11] and other references therein. From Fig. 10, the stability margin parameter, μ, corresponding to the maximum value over frequency of the structured singular value, is 1.28 with the centralized controller and 1.39 with the partitioned controller. These values of μ translate into guaranteed multivariable gain margins of -5.0 dB to 13.2 dB and -4.7 dB to 11.1 dB for the closed-loop

system with the centralized and partitioned controllers, respectively, and similarly guaranteed multivariable phase margins of ±45.9 deg and ±42.2 deg, respectively, for *simultaneous* gain or phase variations occurring in all the loops at the controlled outputs. These results demonstrate that the robustness characteristics of the centralized controller are maintained by the partitioned controllers obtained by application of the stepwise controller partitioning procedure.

Conclusions

A systematic stepwise procedure was presented for partitioning a centralized Integrated Flight Propulsion Control (IFPC) law into decentralized airframe and engine subsystem controllers (subcontrollers) which are coupled through a hierarchical structure. The procedure emphasizes matching the closed-loop performance and robustness characteristics of the centralized controller with the partitioned subcontrollers. The controller partitioning is motivated by implementation issues where it is desirable to perform independent performance validation of each subsystem while guaranteeing that the desired vehicle performance will be achieved on subsystem integration. The steps in the procedure were described and demonstrated through application to IFPC design for a Short Take-Off and Vertical Landing aircraft in the landing approach to hover transition flight phase. For the example application, the controller partitioning procedure resulted in highly structured low order airframe and engine subcontrollers that maintain the command tracking and decoupling performance achieved by the centralized controller. The partitioned subcontrollers were also shown to have multivariable stability margins similar to the centralized controller for gain and phase variations reflected at the controlled outputs.

Appendix

Numerical Data

The system (plant and controller) state-space matrices are listed in the following in the standard form :

$$S = \begin{bmatrix} A & | & B \\ -- & | & -- \\ C & | & D \end{bmatrix}$$

The plant system matrix, S_p, with the outputs $\bar{y} = [V,\dot{V},\theta,q,\gamma,N2,FG9,FGE,FGV]^T$ is

$$S_p = \left[\begin{array}{cccccccccc}
-5.52 & 3.75 & 5.35e-01 & 1.93e-01 & 3.26e-01 & -2.34e-01 & -7.55e-01 & -1.33e-01 & 0 & -1.30e-03 \\
5.13e-01 & -3.85 & 8.07e-01 & 2.83e-01 & -8.11e-02 & 1.03e-02 & 4.49e-03 & 7.90e-04 & 0 & 7.76e-06 \\
1.54e-02 & 7.99e-03 & -2.38e-01 & 5.27e-04 & 3.37e-04 & 6.00e-04 & 3.91e-03 & 6.88e-04 & 0 & 6.76e-06 \\
1.34e-03 & -5.52e-03 & 1.29e-02 & -8.38e-02 & 1.23e-04 & 1.44e-04 & -1.44e-03 & -2.53e-04 & 0 & -2.48e-06 \\
1.57e-03 & -3.51e-02 & 2.47e-02 & 8.29e-03 & -1.81e-01 & 4.21e-04 & -5.93e-03 & -1.04e-03 & 0 & -1.02e-05 \\
2.96e-03 & -1.43e-02 & 8.40e-03 & 2.36e-03 & 5.85e-03 & -8.35e-02 & -1.23e-03 & -2.16e-04 & 0 & -2.12e-06 \\
1.87e-03 & 5.15e-04 & 5.44e-05 & -4.33e-05 & 2.24e-05 & 1.48e-04 & -5.79e-02 & 7.20e-02 & -2.28e+01 & -3.19e+01 \\
-5.48e-03 & -1.41e-03 & -8.43e-05 & 1.21e-04 & -4.66e-05 & -3.46e-04 & -1.42e-01 & -4.04e-01 & 1.30e+02 & -3.92 \\
2.05e-04 & 5.28e-05 & 3.77e-06 & -4.30e-06 & 2.09e-06 & 1.35e-05 & -1.22e-02 & 1.89e-02 & -5.48e-01 & 1.54e-07 \\
0 & 0 & 0 & 0 & 0 & 0 & 0 & 0 & 1.0 & 0 \\
0 & 0 & 0 & 0 & 0 & 0 & 1.22e-01 & -9.92e-01 & 0 & 1.35e+02 \\
\hline
-3.96e-06 & -1.02e-06 & 0 & 0 & 0 & -2.49e-07 & 9.85e-01 & 1.73e-01 & 0 & 1.53e-03 \\
8.97e-04 & 2.63e-04 & 3.90e-05 & -2.16e-05 & 1.39e-05 & 8.54e-05 & -8.16e-02 & 9.42e-04 & 7.37e-05 & -3.21e+01 \\
0 & 0 & 0 & 0 & 0 & 0 & 0 & 0 & 0 & 5.73e+01 \\
0 & 0 & 0 & 0 & 0 & 0 & 0 & 0 & 5.73e+01 & 0 \\
0 & 0 & 0 & 0 & 0 & 0 & 7.35e-02 & -4.18e-01 & 0 & 5.73e+01 \\
1.0 & 0 & 0 & 0 & 0 & 0 & 0 & 0 & 0 & 0 \\
6.66e-01 & 1.71e-01 & 1.00e-02 & -1.53e-02 & 5.13e-03 & 4.16e-02 & 2.98e-01 & 5.24e-02 & 0 & 5.14e-04 \\
1.33 & 3.46e-01 & 2.42e-02 & -2.88e-02 & 1.29e-02 & 8.79e-02 & 5.97e-01 & 1.05e-01 & 0 & 1.03e-03 \\
1.94 & 5.00e-01 & 2.91e-02 & -4.39e-02 & 1.59e-02 & 1.22e-01 & 8.69e-01 & 1.53e-01 & 0 & 1.50e-03
\end{array}\right]$$

1.32e-01	0	0	-2.76e-01	-7.07e-02	3.36e-01	2.56e+01	4.77e+01	2.43e+01
5.62e-02	0	0	-1.33e-01	-4.48e-02	7.13e-01	-3.02	-6.18	-2.87
-5.13e-04	0	0	-1.17e-04	-2.93e-05	1.26e-03	-7.38e-02	-1.40e-01	-7.00e-02
8.20e-04	0	0	-5.76e-04	-1.64e-04	6.46e-03	-1.94e-02	-3.97e-02	-1.84e-02
2.99e-03	0	0	-1.73e-03	-5.32e-04	2.20e-02	-5.45e-02	-1.13e-01	-5.19e-02
9.25e-04	0	0	1.54e-04	2.05e-05	7.09e-03	-4.91e-02	-9.46e-02	-4.66e-02
6.05e-06	-3.18e-02	-1.52e-01	-1.95e-01	-5.23e-04	1.56e-04	3.27e-02	-1.01e-01	-2.81e-03
6.36e-04	-2.13e-01	-3.52e-01	-7.73e-02	-8.72e-02	-3.60e-04	5.28e-02	-1.45e-01	1.17e-02
1.22e-05	-2.34e-02	2.56e-01	-1.68e-02	-2.15e-02	1.37e-05	-1.25e-03	3.08e-02	-3.71e-03
0	0	0	0	0	0	0	0	0
-1.00e-04	0	-4.05e-06	0	0	0	-6.26e-07	5.43e-06	-5.93e-07
---	---	---	---	---	---	---	---	---
1.69e-07	0	-2.87e-04	8.05e-05	-2.95e-07	-2.62e-07	3.87e-05	7.04e-05	-1.26e-05
1.16e-04	-3.41e-02	-2.11e-01	-2.06e-01	-1.56e-02	9.08e-05	4.14e-02	-1.25e-01	-7.31e-04
0	0	0	0	0	0	0	0	0
0	0	0	0	0	0	0	0	0
-1.67e-06	0	-8.24e-06	1.89e-06	0	0	6.72e-07	3.69e-06	-5.18e-07
0	0	0	0	0	0	0	0	0
-3.45e-02	0	0	1.71e-01	5.05e-02	4.39e-02	2.30e+01	-1.18e+01	-6.16
-4.85e-02	0	0	3.44e-01	1.02e-01	9.06e-02	-1.31e+01	1.14e+02	-1.24e+01
-8.29e-02	0	0	4.94e-01	1.45e-01	1.28e-01	-1.90e+01	-3.45e+01	6.20

The bleed flow is given by WB3=4.41|AQR|.

The centralized controller system matrix, S_K, with the inputs and outputs ordered as defined in equation (4), is

$$S_K = \begin{bmatrix}
-3.50e-03 & -3.20e-03 & -7.59e-03 & -1.00e-03 & -5.33e-03 & -6.00e-04 & 3.97e-04 \\
6.82e-04 & -5.60e-03 & -2.92e-02 & -3.76e-03 & -1.91e-02 & -2.14e-03 & 1.44e-03 \\
6.31e-03 & 1.44e-02 & -1.57e-01 & -3.34e-02 & -2.35e-01 & -2.62e-02 & 1.71e-02 \\
8.24e-04 & 2.07e-03 & -1.85e-02 & -6.66e-03 & -7.06e-02 & -8.82e-03 & 3.40e-03 \\
-2.20e-03 & -7.29e-03 & 9.21e-02 & 4.66e-02 & -1.13 & -1.57e-01 & 1.80e-01 \\
-2.25e-04 & -7.51e-04 & 9.51e-03 & 4.94e-03 & -1.21e-01 & -2.43e-02 & 1.10e-02 \\
2.91e-06 & -1.50e-03 & 8.28e-03 & 1.65e-03 & -1.46e-01 & -2.02e-02 & -2.21e-01 \\
-1.18e-03 & -9.49e-03 & 9.53e-02 & 3.91e-02 & 8.73e-02 & 6.53e-03 & 5.19 \\
5.71e-04 & 3.87e-04 & -1.56e-02 & -8.74e-03 & 1.95e-01 & 2.65e-02 & 2.13e-01 \\
-1.19e-04 & 8.87e-04 & -9.58e-03 & -4.65e-04 & -2.74e-01 & -3.84e-02 & -1.16e-01 \\
--- & --- & --- & --- & --- & --- & --- \\
-1.34e-01 & -1.19e-01 & -1.12e-01 & -5.12e-02 & -1.10e-01 & -1.27e-01 & 9.90e-02 \\
-1.37e-03 & 1.91e-03 & -2.27e-04 & -3.66e-03 & 1.40e-03 & 1.03e-03 & -1.89e-02 \\
-4.60e-02 & 4.95e-02 & 1.58e-01 & -5.27e-01 & 4.36e-02 & 2.73e-02 & -1.24e-01 \\
-2.04e-01 & -1.51e-01 & -1.97e-01 & -2.86e-01 & -1.18e-01 & -1.76e-01 & 2.66e-01 \\
-2.10e+01 & -9.37 & -2.20e+01 & -2.94 & -1.60e+01 & -1.75 & 1.26 \\
5.54e-01 & 2.04e-01 & 3.64e-01 & 6.88e-01 & 3.41e-01 & 4.63e-01 & 3.57e-01 \\
-1.94e-01 & -1.76e-02 & -9.48e-02 & -3.61e-01 & -6.99e-02 & -5.49e-02 & -4.42e-01 \\
9.61e-01 & 3.83e-01 & 9.80e-01 & 6.36e-01 & 6.10e-01 & 1.05 & 1.16
\end{bmatrix}$$

4.49e-03	7.97e-04	2.44e-04	1.64e+01	8.13	-1.03e+01	-3.46e-03
1.61e-02	2.86e-03	8.63e-04	-3.73	8.27	2.35	-1.18e-02
1.92e-01	3.42e-02	1.04e-02	-1.56e+01	-1.54e+01	4.81e-01	-3.53e-01
5.36e-02	8.97e-03	5.21e-03	-8.66e-01	-2.49	1.64	-1.33e-01
1.90	3.35e-01	1.03e-01	-4.95e-01	8.93	-7.27	-2.44
2.73e-01	4.44e-02	4.48e-02	-7.66e-02	9.87e-01	-7.87e-01	-2.69e-01
-6.49	-4.70e-01	3.25e-01	-2.22e-01	1.16	5.77e-01	-1.85e-01
-1.40e+01	-6.45	-2.31	-5.27e-01	9.09	-9.27e-01	2.17
4.35	-1.34	-1.14	-3.56e-01	-1.11	2.05	-2.90e-02
4.12	1.51	-3.90	-2.46e-01	-5.29e-01	-1.53	-4.83e-01
-1.27e-01	-4.28e-02	-1.99e-02	7.57e-04	-6.80e-03	-5.96e-02	-1.93e-02
2.82e-02	-2.41e-03	1.02e-02	-1.02e-04	4.61e-04	3.79e-03	1.24e-03
-2.05e-01	-3.51e-01	-1.13e-01	-1.84e-03	1.24e-03	1.08e-02	3.80e-03
-1.45e-01	-3.24e-01	6.32e-01	2.04e-04	1.12e-03	1.49e-02	4.65e-03
1.35e+01	2.41	5.99e-01	1.28	7.76	2.13e+01	7.41
-2.99e-01	-1.53e-02	-3.71e-01	1.09e-03	1.91e-02	1.02e-01	3.40e-02
4.27e-01	-1.44e-01	4.25e-01	-1.38e-03	7.47e-03	5.73e-02	1.88e-02
-1.11	4.81e-02	-2.55	-2.16e-03	3.71e-02	2.92e-01	9.52e-02

-4.24e-03	8.58e-03	1.11e-02	1.73e-03	-5.29e-01	6.37e-04	2.91e-03
-1.52e-02	3.06e-02	3.95e-02	6.78e-03	-5.02e-01	2.24e-03	1.02e-02
-4.56e-01	9.10e-01	1.18	2.01e-01	9.79e-02	1.05e-02	9.17e-02
-1.72e-01	3.44e-01	4.44e-01	7.59e-02	2.19e-02	1.04e-03	2.26e-02
-3.16	6.30	8.15	1.39	-2.31e-01	-3.73e-02	4.72e-01
-3.48e-01	6.93e-01	8.97e-01	1.53e-01	1.14	-4.72e-03	6.46e-02
-2.36e-01	4.76e-01	6.16e-01	1.05e-01	5.94e-02	1.45e-01	-9.45e-01
2.81	-5.59	-7.23	-1.23	5.78e-02	9.97e-02	-1.26
-3.85e-02	7.46e-02	9.57e-02	1.64e-02	-2.03e-02	-1.30e-01	6.55e-01
-6.25e-01	1.25	1.61	2.75e-01	4.37e-02	-1.20e-01	-1.90e-01
-2.52e-02	4.98e-02	6.48e-02	1.10e-02	1.21e-03	1.21e-02	-6.84e-02
1.61e-03	-3.21e-03	-4.16e-03	-7.08e-04	-7.86e-05	-9.37e-04	4.11e-03
4.43e-03	-9.79e-03	-1.22e-02	-2.16e-03	-4.83e-04	-5.26e-03	-3.47e-03
6.02e-03	-1.20e-02	-1.56e-02	-2.65e-03	-3.61e-04	-2.52e-03	1.90e-03
9.53	-1.91e+01	-2.47e+01	-4.22	1.24	-3.42	4.40e+01
4.55e-02	-8.78e-02	-1.16e-01	-1.94e-02	3.50e-05	-3.27e-02	5.31e-01
2.39e-02	-4.86e-02	-6.28e-02	-1.07e-02	-9.81e-04	-2.10e-02	1.06e-01
1.23e-01	-2.46e-01	-3.19e-01	-5.43e-02	-4.62e-03	-9.87e-02	8.44e-01

Prior to applying the controller partitioning procedure, the inputs and outputs of the subcontrollers were normalized using the form $\bar{u}_s = [\mathrm{diag}\{\bar{u}_{max}\}]^{-1} \cdot \bar{u}$ where, for example, $\bar{u}_s$ is the vector of scaled variables corresponding to $\bar{u}$. The numerical scaling values for the various subcontroller inputs and outputs defined in equation (2) are listed in the following.

$$\bar{u}_{a\,max} = [5.0,\ 0.7,\ 10.0,\ 10.0]^T$$
$$\bar{u}_{e\,max} = [1000,\ 20,\ 8,\ 45]^T$$
$$\bar{e}_{a\,max} = [7.6,\ 6.3,\ 4.0]^T$$
$$\bar{y}_{a\,max} = [20,\ 6,\ 10,\ 6,\ 4]^T$$
$$\bar{e}_{ea\,max} = [1000,\ 2000,\ 1000]^T$$
$$\bar{e}_{e\,max} = 200$$
$$\bar{y}_{e\,max} = [200,\ 7]^T$$

The system matrices for the subcontrollers $\tilde{K}^a$, K_{ea}^e, and K_e^e obtained using the controller partitioning procedure are listed in the following. These system matrices correspond to the normalized inputs and outputs.

$$S_{K_e^a} = \left[\begin{array}{cccc|ccc} -7.25e\text{-}03 & 3.41e\text{-}04 & 1.88e\text{-}03 & 3.30e\text{-}04 & -2.03 & 9.27e\text{-}04 & 2.60e\text{-}04 \\ -3.67e\text{-}03 & -1.45e\text{-}02 & -3.63e\text{-}02 & -6.24e\text{-}02 & -5.12e\text{-}01 & -4.16e\text{-}02 & -8.79e\text{-}03 \\ -6.45e\text{-}03 & -3.85e\text{-}02 & -1.30e\text{-}01 & -3.11e\text{-}01 & -9.00e\text{-}01 & -1.52e\text{-}01 & -4.51e\text{-}02 \\ 6.83e\text{-}03 & 5.26e\text{-}02 & 2.59e\text{-}01 & 2.93 & 9.56e\text{-}01 & -5.20e\text{-}01 & -3.31e\text{-}01 \\ \hline -1.67 & 1.61e\text{-}01 & 4.95e\text{-}01 & 2.78e\text{-}01 & 2.49e\text{-}01 & -6.83e\text{-}01 & 3.08e\text{-}01 \\ -3.50e\text{-}01 & -3.24e\text{-}01 & -4.99e\text{-}01 & -4.38e\text{-}01 & 3.50e\text{-}04 & -3.27e\text{-}01 & 1.86e\text{-}01 \\ -7.37e\text{-}01 & 2.09e\text{-}01 & 3.40e\text{-}01 & 6.07e\text{-}01 & -2.45e\text{-}02 & -5.24e\text{-}01 & 9.25e\text{-}02 \\ -8.19e\text{-}01 & -3.00e\text{-}01 & -4.75e\text{-}01 & -8.09e\text{-}01 & -2.05e\text{-}02 & -4.39e\text{-}01 & 1.31e\text{-}01 \end{array}\right]$$

$$S_{K_e^e} = \left[\begin{array}{ccc|ccc} -1.09e\text{-}02 & 4.11e\text{-}05 & -6.84e\text{-}06 & 4.93e\text{-}01 & 1.51 & 2.15 \\ 4.89e\text{-}05 & -1.07e\text{-}02 & 7.69e\text{-}06 & -2.49 & 6.74e\text{-}01 & 8.46e\text{-}02 \\ -1.37e\text{-}05 & 1.02e\text{-}05 & -1.07e\text{-}02 & 4.54e\text{-}01 & 1.85 & -1.41 \\ \hline 1.91 & -6.84e\text{-}01 & 1.34e\text{-}01 & 0 & 0 & 0 \\ -1.48 & -1.88 & 6.39e\text{-}01 & 0 & 0 & 0 \\ -2.91e\text{-}01 & 1.27 & 1.96 & 0 & 0 & 0 \\ -1.09 & 1.04 & -1.16 & 0 & 0 & 0 \end{array}\right]$$

$S_{R^3} =$

-3.55e-03	2.69e-03	-1.26e-03	-6.84e-03	-4.92e-03	3.93e-04	-1.07e-03	-1.13e-03
-5.10e-04	-6.75e-03	1.10e-03	2.31e-02	1.35e-02	-8.95e-03	2.57e-03	2.07e-03
4.38e-04	5.13e-05	-3.14e-03	-1.25e-02	-9.21e-03	4.37e-03	-1.31e-02	-2.34e-03
6.93e-03	-9.66e-03	5.35e-03	-1.60e-01	-2.20e-01	4.45e-02	-1.41e-02	-6.07e-02
-1.24e-03	9.39e-03	1.64e-03	8.27e-02	-8.98e-01	2.00e-01	-2.63e-01	-4.05e-01
1.80e-03	-1.06e-02	-3.03e-03	-1.18e-01	-2.56e-01	-2.59	2.48	2.43e-01
-2.78e-04	8.01e-03	-3.65e-03	6.69e-02	9.03e-01	3.54	-6.22	-2.61e-01
7.44e-04	-6.94e-03	-4.12e-03	-4.07e-02	6.20e-01	-1.60	1.16	-2.13
-7.00e-04	4.67e-03	1.91e-03	3.89e-02	-3.89e-01	1.17	-9.55e-01	1.71
---	---	---	---	---	---	---	---
-1.56	1.07	-2.18e-01	-1.54	-1.24	6.63e-01	-4.91e-01	1.74e-01
-1.27e-01	-1.46e-01	3.94e-02	-5.33e-02	-9.17e-02	-9.43e-01	9.03e-01	-2.72e-01
-4.23e-01	-5.75e-01	-4.77e-01	5.11e-01	2.41e-02	-9.83e-02	-1.10	9.58e-02
-1.24	5.53e-01	-3.29e-01	-1.49	-7.02e-01	6.91e-01	-7.15e-01	-7.27e-01
4.58e-01	8.73e-03	1.04e-01	2.35e-01	2.93e-01	1.72e-01	-1.17e-01	-1.55e-01
-1.36	1.33e-01	-6.67e-02	-1.24	-1.01	-1.02	7.69e-01	-3.18e-01
-1.88e-01	1.73e-01	-3.10e-03	-2.09e-01	-1.20e-01	4.64e-01	-2.00e-01	-3.09e-02

7.66e-04	2.26	9.31e-01	-5.33e-01	-1.74e-03	-6.51e-04	2.18e-03	1.69e-03	1.83e-04
-2.11e-03	5.75e-01	-1.22	1.55e-01	9.57e-04	3.69e-04	-1.26e-03	-9.68e-04	-1.15e-04
1.10e-03	-3.96e-02	1.23e-01	6.19e-01	-4.14e-03	-1.60e-03	5.33e-03	4.13e-03	4.70e-04
4.42e-02	-1.96	-1.61	5.28e-02	-1.17e-01	-4.53e-02	1.51e-01	1.17e-01	1.33e-02
2.86e-01	-1.82e-02	1.01	-3.65e-01	-7.24e-01	-2.81e-01	9.33e-01	7.24e-01	8.25e-02
-1.28e-01	-9.62e-02	-1.17	5.19e-01	-6.16e-01	-2.39e-01	7.94e-01	6.16e-01	7.02e-02
-2.07e-01	-1.83e-01	8.42e-01	2.24e-01	8.28e-01	3.22e-01	-1.07	-8.29e-01	-9.43e-02
1.28	1.12e-01	-6.52e-01	5.64e-01	5.46e-02	2.06e-02	-7.05e-02	-5.46e-02	-6.24e-03
-1.17	2.69e-03	4.86e-01	-2.94e-01	-1.67e-02	-5.91e-03	2.15e-02	1.65e-02	1.91e-03
---	---	---	---	---	---	---	---	---
-3.15e-02	1.15e-03	-8.57e-03	-4.77e-02	-7.73e-02	-3.02e-02	9.96e-02	7.78e-02	8.81e-03
2.24e-01	-1.10e-03	4.15e-03	2.17e-02	3.55e-02	1.38e-02	-4.58e-02	-3.57e-02	-4.05e-03
-1.58e-01	-1.40e-03	7.81e-04	4.33e-03	7.59e-03	2.66e-03	-9.79e-03	-7.35e-03	-8.65e-04
4.66e-01	1.55e-04	7.07e-04	5.95e-03	9.29e-03	3.61e-03	-1.20e-02	-9.33e-03	-1.06e-03
1.58e-02	8.40e-04	2.92e-03	3.17e-03	5.96e-03	2.54e-03	-7.70e-03	-6.26e-03	-6.81e-04
1.51e-01	-1.09e-04	2.65e-03	6.95e-03	1.18e-02	4.39e-03	-1.53e-02	-1.17e-02	-1.35e-03
-8.51e-02	1.34e-03	3.81e-03	2.53e-03	4.90e-03	1.76e-03	-6.31e-03	-4.69e-03	-5.57e-04

References

1. Sandell, N.R., Jr., et al.: Survey of Decentralized Control Methods for Large Scale Systems. IEEE Trans. Autom. Control, vol. AC-23, no. 2, Apr. 1978, pp. 108-128.

2. Shaw, P.D., et al.: Design Methods for Integrated Control Systems. Report AFWAL-TR-88-2061, Wright Patterson AFB, OH, June 1988.

3. Mattern, D.L.; Garg, S.; and Bullard, R.E.: Integrated Flight/Propulsion Control System Design Based on a Centralized Approach. AIAA Paper 89-3519, 1989.

4. Smith, K.L.: Design Methods for Integrated Control Systems. Report AFWAL-TR-86-2103, Wright Patterson AFB, OH, Dec. 1986.

5. Garg, S.; Mattern, D.L.; and Bullard, R.E.: Integrated Flight/Propulsion Control System Design Based on a Centralized Approach. J. Guid. Control Dyn., vol. 14, no. 1, Jan.-Feb. 1991, pp. 107-116.

6. Garg, S., et al.: IMPAC - an Integrated Methodology for Propulsion and Airframe Control. 1991 American Control Conference, 10th; Proceedings, Vol. 1, IEEE, New York, 1991, pp. 747-754.

7. Moore, B.C.: Principal Component Analysis in Linear Systems: Controllability, Observability, and Model Reduction. IEEE Trans. Autom. Control, vol. AC-26, Feb. 1981, pp. 17-31.

8. Garg, S.; and Ouzts, P.J.: Integrated Flight/Propulsion Control Design for a STOVL Aircraft using H-Infinity Control Design Techniques. 1991 American Control Conference, 10th; Proceedings, Vol. 1, IEEE, New York, 1991, pp. 568-576.

9. Garg, S.; and Mattern, D.L.: Application of an Integrated Flight/Propulsion Control Design Methodology to a STOVL Aircraft. AIAA Paper 91-2792, 1991.

10. Safonov, M.G.; and Chiang, R.Y.: CACSD Using the State-Space L_∞ Theory - A Design Example. IEEE Trans. Autom. Control, vol. AC-33, May 1988, pp. 477-479.

11. Apkarian, P.R.: Structured Stability Robustness Improvement by Eigenspace Assignment Techniques: A Hybrid Methodology. J. Guid. Control Dyn., vol. 12, no. 2, Mar.-Apr. 1989, pp. 162-168.

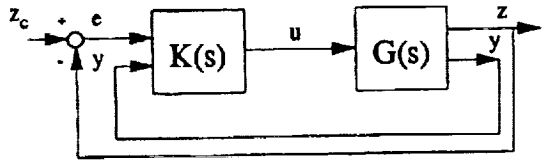

Centralized Control Loop

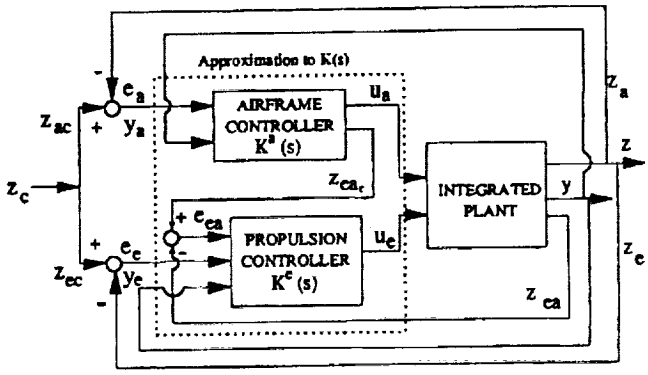

Decentralized, Hierarchically partitioned control loop

Figure 1.—Controller partitioning structure.

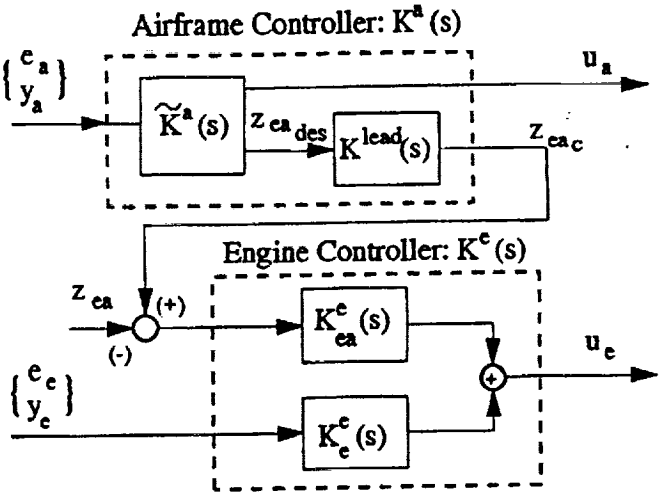

Figure 2.—Detailed structure of partitioned subcontrollers.

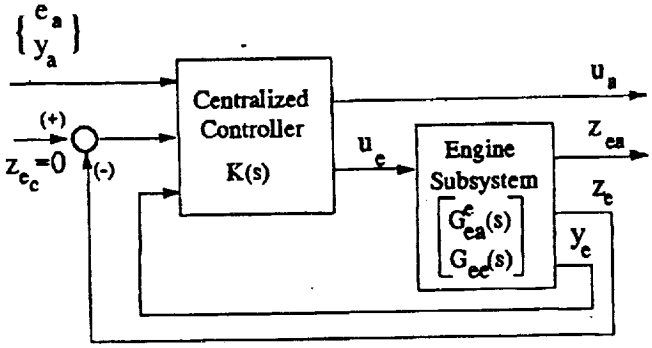

Figure 3.—Control loop to determine $\bar{K}^{ea}(s)$ block of partitioned airframe subcontroller.

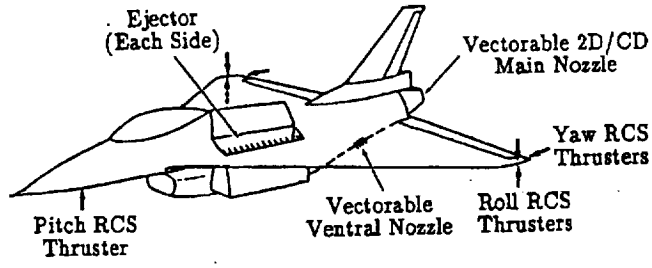

Figure 4.—Control effectors for E-7D aircraft.

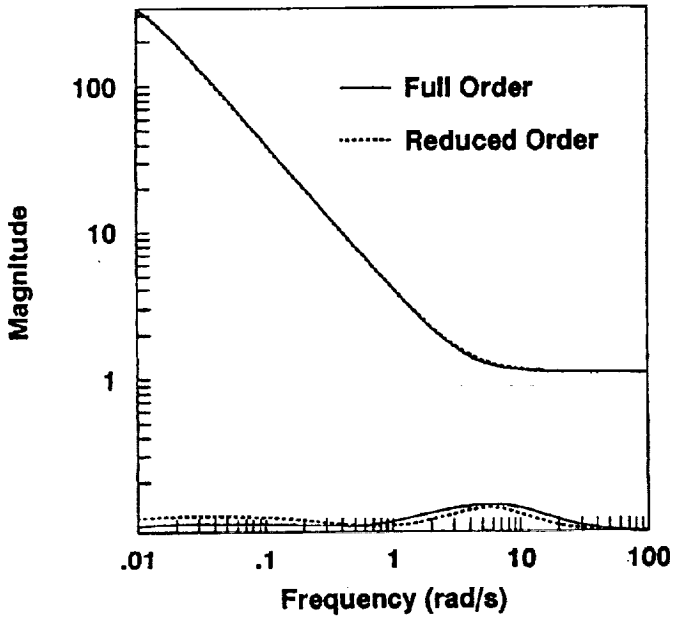

Figure 5.—Maximum and minimum singular values of the $K_{ee}(s)$ portion of the centralized controller - full order (10), and reduced order (4) approximation.

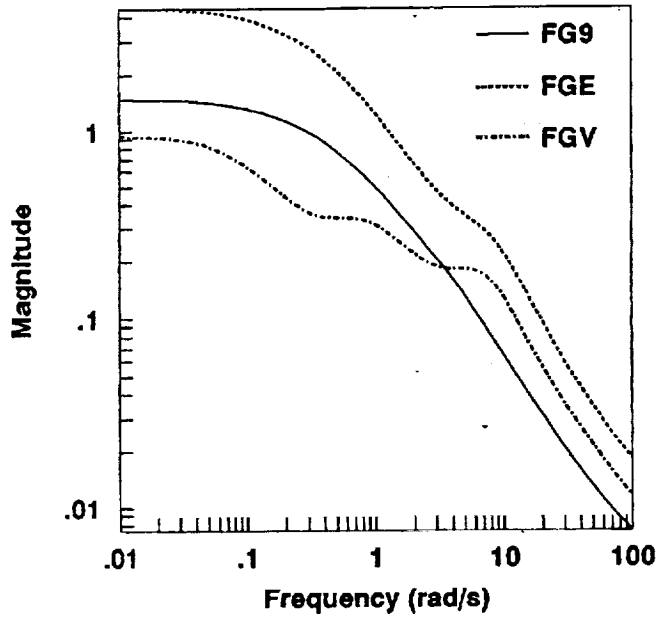

Figure 6.—Thrust requirements $\left(\sigma\left[T^{ea}_{a_c i}(j\omega)\right]\right)$ for tracking the airframe commands $\bar{z}_{a_c}$ with the centralized controller.

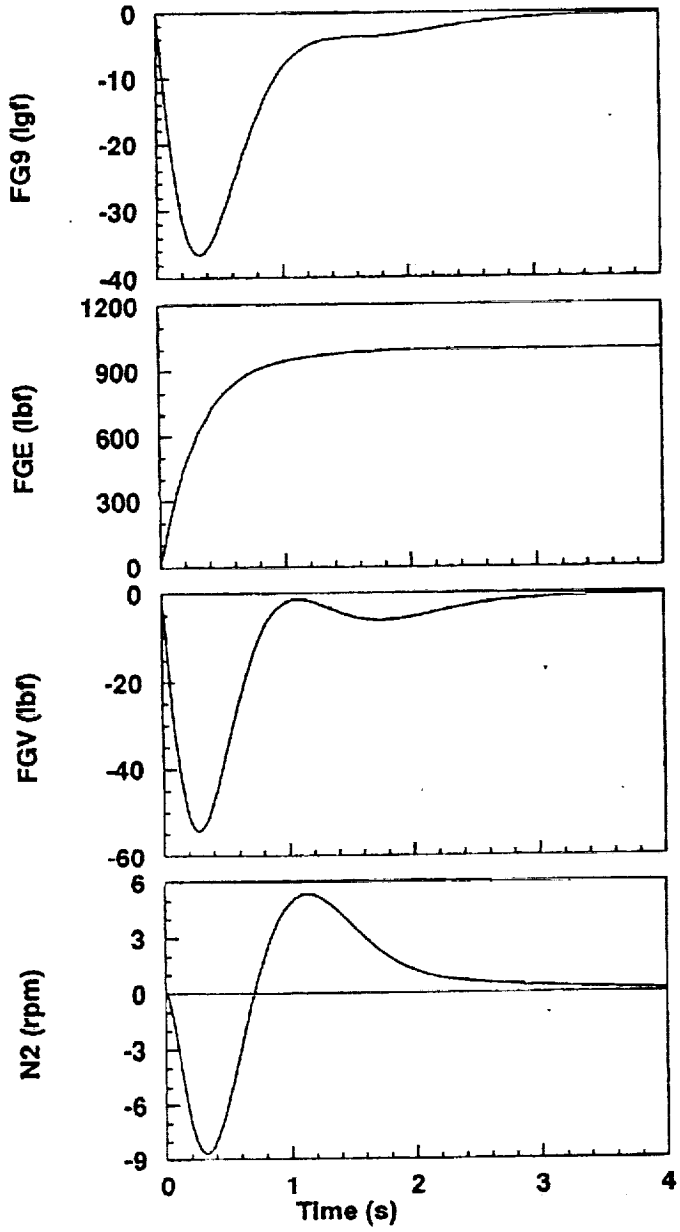

Figure 7.—Engine subsystem closed-loop response to step FGE $_c$ = 1000 lbf with partitioned subcontrolled K ^{e}(s).

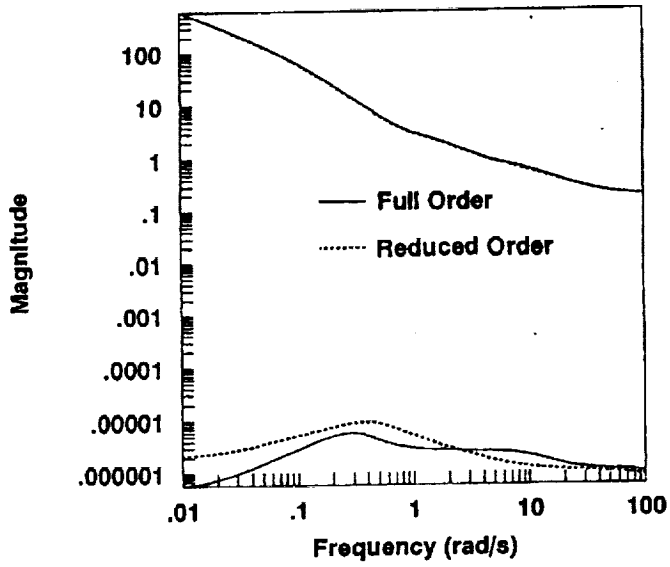

Figure 8.—Maximum and minumum singular values for $\left[\bar{e}_a / \bar{y}_a\right] \rightarrow \left[\bar{u}_a / \bar{z}_{ea}\right]$ response with the centralized controller - full order (16), and reduced order (9) approximation.

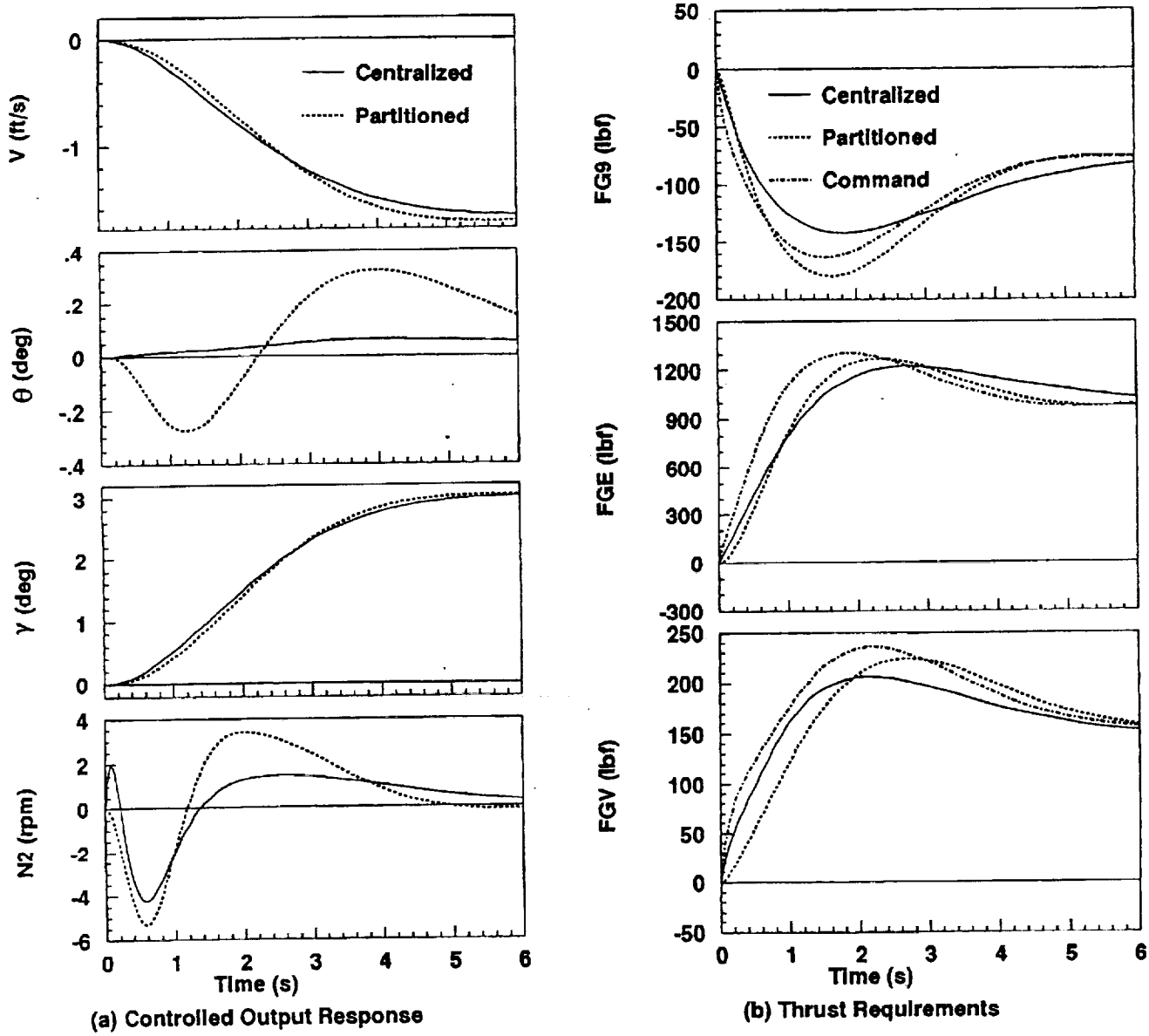

Figure 9.—Closed-loop system response to step γ_c = 3 degrees with centralized and partitioned controllers.

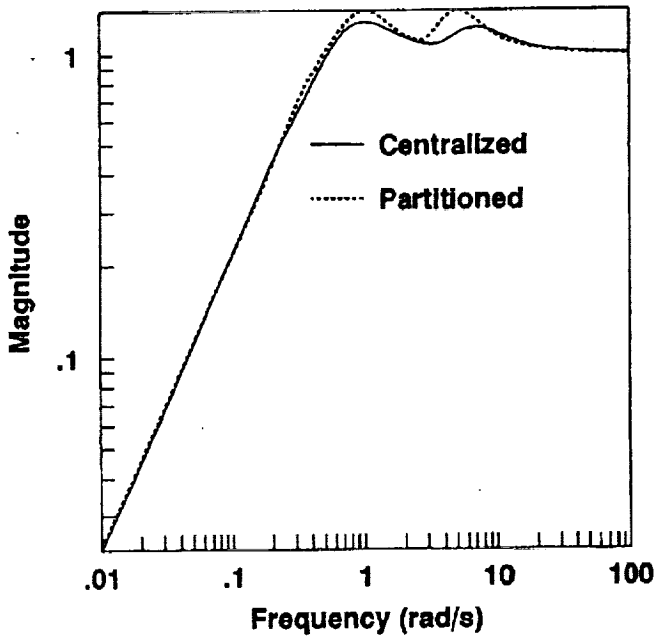

Figure 10.—Structured singular value for robustness analysis to gain and phase variations at the controlled outputs $\bar{z}$ with centralized and partitioned controllers.

REPORT DOCUMENTATION PAGE

Form Approved
OMB No. 0704-0188

1. AGENCY USE ONLY (Leave blank)	2. REPORT DATE	3. REPORT TYPE AND DATES COVERED
	February 1993	Technical Memorandum

4. TITLE AND SUBTITLE
Controller Partitioning for Integrated Flight/Propulsion Control Implementation

5. FUNDING NUMBERS
WU-505-62-50

6. AUTHOR(S)
Sanjay Garg

7. PERFORMING ORGANIZATION NAME(S) AND ADDRESS(ES)
National Aeronautics and Space Administration
Lewis Research Center
Cleveland, Ohio 44135-3191

8. PERFORMING ORGANIZATION REPORT NUMBER
E-7234

9. SPONSORING/MONITORING AGENCY NAMES(S) AND ADDRESS(ES)
National Aeronautics and Space Administration
Washington, D.C. 20546-0001

10. SPONSORING/MONITORING AGENCY REPORT NUMBER
NASA TM-105804

11. SUPPLEMENTARY NOTES
Prepared for the 1992 American Control Conference sponsored by the American Automatic Control Council, Chicago, Illinois, June 24-26, 1992.

12a. DISTRIBUTION/AVAILABILITY STATEMENT
Unclassified - Unlimited
Subject Categories 08 and 63

12b. DISTRIBUTION CODE

13. ABSTRACT *(Maximum 200 words)*

The notion of partitioning a centralized controller into a decentralized, hierarchical structure suitable for integrated flight/propulsion control (IFPC) implementation is discussed. A systematic procedure is developed for determining partitioned airframe and engine subsystem controllers (subcontrollers), with the desired interconnection structure, that approximate the closed-loop performance and robustness characteristics of a given centralized controller. The procedure is demonstrated by application to IFPC design for a Short Take-Off and Vertical Landing (STOVL) aircraft in the landing approach to hover transition flight phase.

14. SUBJECT TERMS
Controller partitioning; Integrated control; Centralized control; Decentralized control

15. NUMBER OF PAGES
28

16. PRICE CODE
A03

17. SECURITY CLASSIFICATION OF REPORT	18. SECURITY CLASSIFICATION OF THIS PAGE	19. SECURITY CLASSIFICATION OF ABSTRACT	20. LIMITATION OF ABSTRACT
Unclassified	Unclassified	Unclassified	